Experiments in Fluids 7, 259–264 (1989)

Experiments in Fluids

Scalar interfaces in digital images of turbulent flows

R. R. Prasad and **K. R. Sreenivasan**
Mason Laboratory, Yale University, New Haven, CT 06520, USA

Abstract. A scalar interface is defined as the surface separating the scalar-marked regions of a turbulent flow from the rest. The problem of determining the two-dimensional intersections of scalar interfaces is examined, taking as a specific example digital images of an axisymmetric jet visualized by laser-induced fluorescence. The usefulness of gradient and Laplacian techniques for this purpose is assessed, and it is shown that setting a proper threshold on the pixel intensity works well if the signal/noise ratio is high. Two methods of determining the proper threshold are presented, and the results are discussed. As one application of the technique, the fractal dimension of the scalar interface is calculated.

1 Introduction

It is of considerable interest to be able to define and determine the vorticity interface, that is the surface separating turbulent regions in a fluid flow from the non-turbulent ones. Similarly, scalar interfaces, defined as surfaces separating the scalar-marked regions from the rest, are also of interest. Two dimensional sections of scalar interfaces – to be called the boundary in the following – have been a central feature of our earlier work (Sreenivasan and Meneveau 1986; Sreenivasan and Prasad 1988) on the determination of the fractal dimension of the interface. The basis of this work is the ability to determine properly the boundary in digital images of the flow, and it is in this context that the present problem arose. We examine here the determination of the boundary in two-dimensional digital images of scalar-marked regions in turbulent jets visualized by laser-induced fluorescence.

Although the problem in this form has not been addressed explicitly before, the equivalent question has been faced for a long time in the determination of outer layer intermittency in hot or cold wire records, especially for conditional measurements. Many different techniques have been used to distinguish turbulent regions from the non-turbulent ones. A review can be found, among other places, in Bradshaw and Murlis (1973), Antonia and Atkinson (1974), Kovasznay and Ali (1974), Antonia et al. (1975), Hedley and Keffer (1974), and Antonia (1981). The most relevant comparison here is with the work involving passive scalars typified by Kovasznay and Ali (1974) and Antonia et al. (1975). Kovasznay and Ali not only used a threshold on the temperature signal to determine the interface, but also resorted to the so-called hold-time, according to which a region is not considered turbulent unless it spans a certain (arbitrarily set) hold-time. Setting a proper hold-time is very difficult, and a unique value that is satisfactory in all contexts is unlikely to exist. Its precise value is not very important for determining gross features such as the intermittency factor (that is, the fraction of time the flow is turbulent), but its effect on small scale features could be quite profound. Antonia et al. (1975) used a threshold without a hold-time, but this led to some difficulties in discriminating small turbulent amplitudes against spurious noise in the non-turbulent regions. Sunyach and Mathieu (1969) used a threshold on the square of the temperature gradient to overcome this problem, but this reintroduces the need for a hold-time.

It should be quite clear from this necessarily brief discussion that there are several problems in properly discriminating turbulent regions in hot and cold wire signals from the non-turbulent ones, and it can be expected that similar problems abound in two-dimensional sections. Determining the boundary in two-dimensional images is similar in several respects to edge detection, which is a well-understood procedure (e.g., Castleman 1979; Rosenfeld and Kak 1982) when the boundaries are sharp. This not being the case in flow visualization pictures, some further considerations are needed. This is the subject of this paper.

2 Experimental set-up

Two-dimensional laser-induced fluorescence visualizations of turbulent jets in water are considered here. Briefly, the jet is produced by allowing filtered water from a well-contoured nozzle of circular cross-section (diameter 12 mm) to flow into a tank of still filtered water (tank size: 80 cm square, 90 cm high). The jet was made visible by mixing a small amount (on the order of 10 ppm) of a fluorescent dye (so-

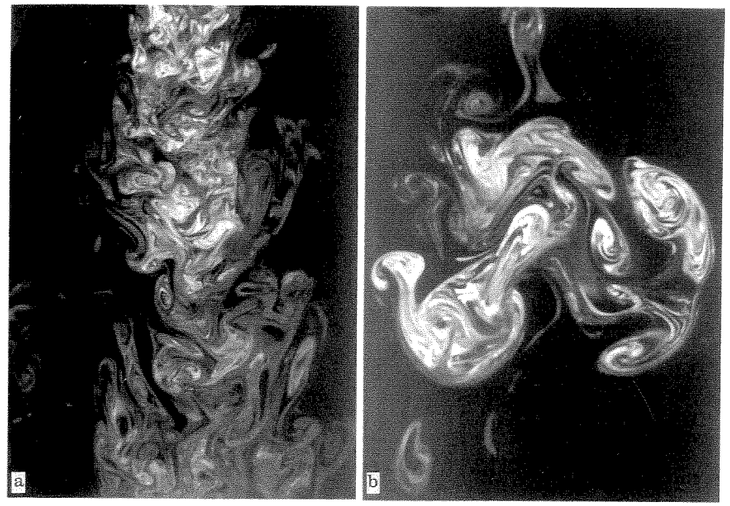

Fig. 1 a and b. Two dimensional sections of an axisymmetric water jet visualized by laser induced fluorescence: **a** axial and **b** orthogonal, x/D = 21; the two pictures do not correspond to the same instant

dium fluorescein) into the nozzle fluid, and exciting fluorescence by illuminating a two-dimensional section of the flow with a sheet of laser radiation produced from a Nd:YAG pulsed laser with a 10 ns pulse width (small enough to freeze the fluid motion) and a maximum power density of 2×10^7 Js^{-1} per pulse. The laser sheet had a thickness of approximately 250 μm, as measured using a linear photodiode array. This being on the order of the estimated Kolmogorov scale (the smallest dynamical scale in the flow), all convolutions of that order have been resolved. (The high Schmidt number of the dye implies that the smallest concentration scales are, however, not resolved.) The jet region, extending from 8 to 24 nozzle diameters, was imaged on to a CCD camera with a 1,300 (vertical) × 1,000 (horizontal) pixel array, yielding a resolution of 150 μm^2. Orthogonal sections at different streamwise stations were also obtained.

To make sure that fluorescence intensity was directly proportional to the concentration of the jet fluid, care was taken that fluorescence was not saturated. This was ascertained, for example, by increasing the dye concentration by a factor of two and observing that the maximum level of intensity also increased by a factor of two. The stray light effects were reduced by using a fresh tank of water for each experimental run lasting no more than necessary for obtaining an image in the steady state of the flow, and by subtracting the background intensity (without laser sheet) from each image. Corrections for nonuniformities due to optical effects and in the laser sheet illumination were made by normalizing each pixel intensity with the corresponding intensity obtained by dyeing the tank fluid uniformly (with no jet running), and illuminating it with the laser sheet.

Figure 1 a and b shows typical realizations of the axial as well as the orthogonal jet sections. Our interest in these two-dimensional images is in determining as faithfully as possible the boundary separating the scalar-mixed areas (the bright regions) from the background.

3 Interface determination

Gradient and Laplacian operators of two-dimensional images are often used to provide edge enhancement (e.g., Rosenfeld and Kak 1982). In the context of Fig. 1, the principle consists in computing the gradient or the Laplacian of the pixel intensity. If the intensity change across the edges is sharp (as would be the case if the pixel intensity is zero within some regions and large in others), this method highlights edges and has been used quite extensively. However, the intensity in actual fluid experiments is not a constant varying between two fixed values, and this leads to complications. We have found that it takes only moderately intense fluctuations for the squared-gradient or the Laplacian of the pixel intensity to introduce false edges.

The problem is illustrated in Fig. 2 by taking a line intersection of the pixel intensity across the jet. The square of its gradient is shown in Fig. 3. It is clear that isolating the boundary of the mixed fluid region is not obvious. While the intensity profile (Fig. 2) shows that the region between pixels 500 and 850 is one region that corresponds to the jet fluid in this profile, the squared gradient operation (Fig. 3) does not show this fact clearly. In fact, if large values of the gradient square are taken to correspond to interfaces, one is forced to conclude that interfaces exist at pixels 750 and 850, implying that the in-between region corresponds to the unmixed tank fluid. A glance at Fig. 2 clearly shows that this is not the case. This problem can no doubt be handled in an ad hoc manner by using a quantity equivalent in spirit to the hold-time, but it should be clear that the arbitrariness involved in this procedure cannot always be justified.

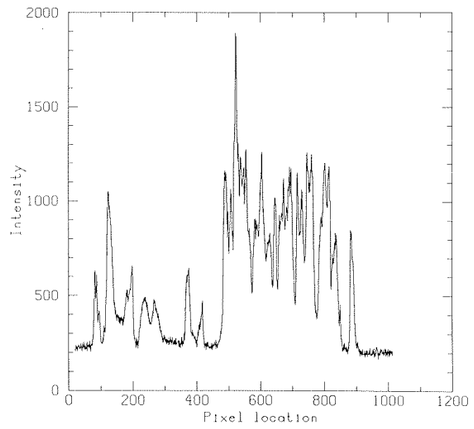

Fig. 2. The pixel intensity profile corresponding to one of the rows of the image shown in Fig. 1

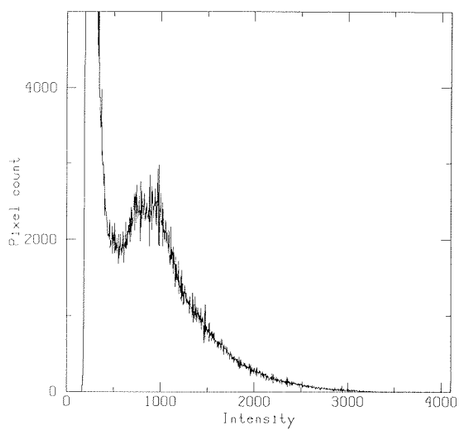

Fig. 4. Histogram of intensities calculated from the image shown in Fig. 1 a; the ordinate is truncated at a pixel count of 5,000 to display clearly regions of higher intensity; the bimodal distribution has a local minimum at pixel intensity of 585

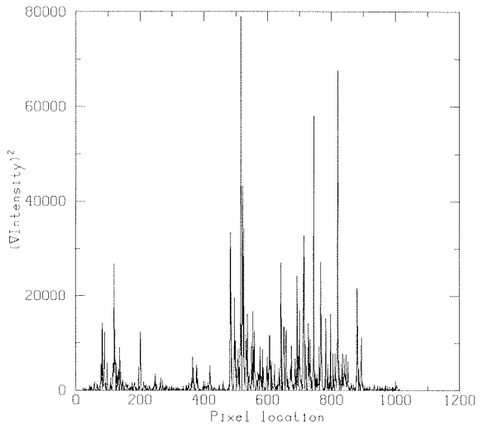

Fig. 3. Square of the gradient of the intensity profile shown in Fig. 2

As remarked already, the Laplacian is also used for edge detection. Again due to the large changes of intensity within the mixed regions the interface is not clearly apparent. Our experience is also that techniques based on spatial filtering (e.g., Marr and Hildreth 1980; Canny 1986) have the problem of smoothing the small scale convolutions which are very important in our considerations.

Looking at the intensity profile of Fig. 2, and the image of the flow (Fig. 1), it is fairly obvious that the pixel intensity is large for regions inside the jet and small for regions outside the jet. From such an intuitive feel comes the idea of using a threshold on the pixel intensity as a means of determining the boundary. The pixel intensity in a two-dimensional image such as Fig. 1 is proportional to the concentration of the jet fluid. For a brief discussion of this point and relevant references see e.g. Dimotakis et al. (1983). A threshold that generates a boundary that circumscribes all the bright areas of the image (Fig. 1) may be chosen by trying a series of different thresholds until the most satisfactory one is found. This method is not new and has been used successfully for data compaction of large images (e.g., Hesselink 1988), but it has the disadvantage of being subjective. Methods of rendering this procedure somewhat objective are now considered.

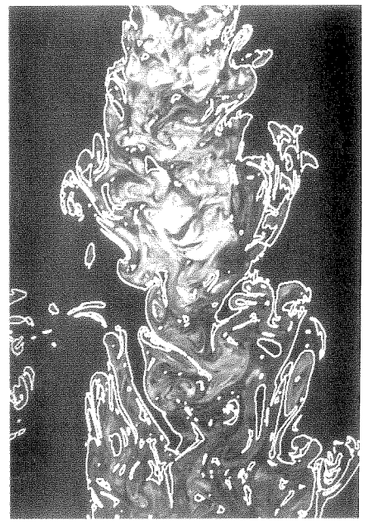

Fig. 5. Computer generated interface (marked by white) of the jet section of Fig. 1 a; the interface was generated using the threshold determined from Fig. 4

Fig. 6. Two-dimensional laser-induced fluorescence visualization of a plane section of the jet taken one diameter off-axis

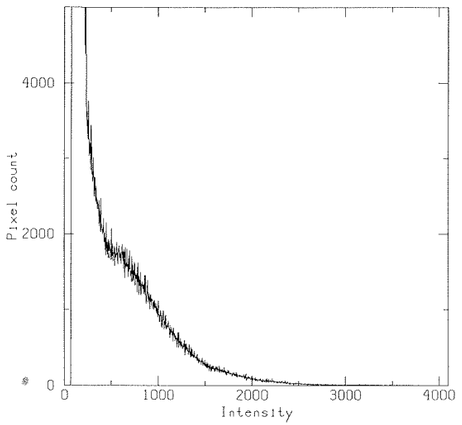

Fig. 7. Histogram of intensities calculated from the image shown in Fig. 6; the ordinate is truncated at a pixel count of 5,000 to display with clarity regions of higher intensity; note that the peaks have merged into one making it impossible to determine the correct threshold by identifying a local minimum

It is clear from Fig. 1 that it contains primarily bright and dark regions, indicating that a histogram of intensities over the entire image could be bimodal (e.g., Rosenfeld and Kak 1982). The peak at the low intensity would correspond to the tank fluid, and that at the high intensity to the jet fluid. Of course, it is to be expected that both peaks would be broadened, the lower one by convolution with background noise and the higher one because of the shades of grey in the mixed fluid, but if a local minimum between the two maxima exists, it could then be a possible threshold. This idea can be made more formal following the general scheme proposed by Bilger et al. (1977) (see also Sreenivasan et al. 1978) for outer layer intermittency determination but the result is effectively the same.

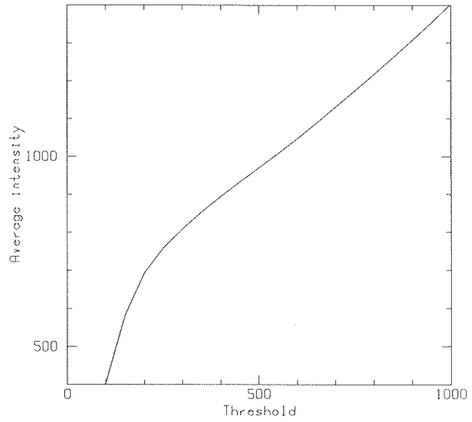

Fig. 8. Thresholded average intensity calculated from the image shown in Fig. 6; note that the slope of the curve changes at a threshold of about 225

Figure 4 shows the histogram of intensities calculated from the image in Fig. 1a. The distribution is sufficiently bimodal in character that the threshold corresponding to the local minimum can be determined unambiguously and applied to the jet. Figure 5 shows that this threshold is adequate. This method was used for several images, and in each case where bimodality is present, it worked well without need for further qualification.

However, histograms of pixel intensity are not always bimodal. Figure 6 shows a visualization of a plane in the axisymmetric jet that is 1 diameter off-axis. It is fairly clear that the darker regions dominate the image, as compared to Fig. 1. The histogram of intensities calculated from this image is shown in Fig. 7. The bright part of the image is a smaller fraction of the entire jet, and the peak in the histogram corresponding to the jet fluid is much smaller than that for the tank fluid. The histogram is not unambiguously bimodal as in Fig. 4. In such cases the threshold can be determined in an objective manner by a different technique consisting of computing the thresholded average intensity (that is, the average intensity over the entire image calculated using only those pixels of intensity above a set threshold) as a function of the threshold. Figure 8 shows this thresholded average intensity curve for the image of Fig. 6. The curve can be seen to have two slopes, with the change occurring at a threshold of 225. This threshold may be obtained numerically by finding the zero crossing of the Laplacian of the thresholded average intensity curve. Figure 9, which marks the boundary computed using this procedure, shows that this is indeed the appropriate threshold.

Fig. 9. Computer generated interface (marked white) of the jet section shown in Fig. 6; the interface was generated using the threshold found from the slope change of the thresholded average intensity curve of Fig. 8

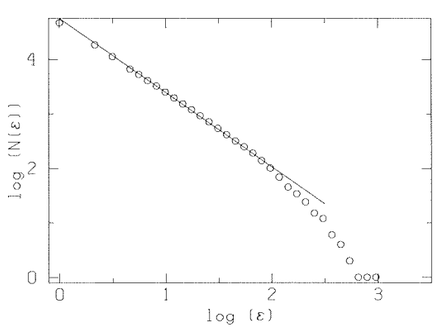

Fig. 10. Log-log plot of the number of boxes $N(\varepsilon)$ containing the boundary vs the size of the box ε; from the straight line portion of the graph the fractal dimension is found to be 1.36

4 Fractal dimension of interfaces

As already remarked, one of our reasons for marking the boundary is the calculation of the fractal dimension (Mandelbrot 1983) of the interface. The reason for expecting the interface to be a fractal is that it is convoluted and fragmented over a wide range of self-similar scales. A primary attribute of fractals is the fractal dimension. The fractal dimension of the surface is rather simply related to that of the boundary in two-dimensional sections if the latter is independent of the orientation of the intersecting plane (Mandelbrot 1983, and references cited there): the dimension of the boundary in intersections is one less than that of the surface itself.

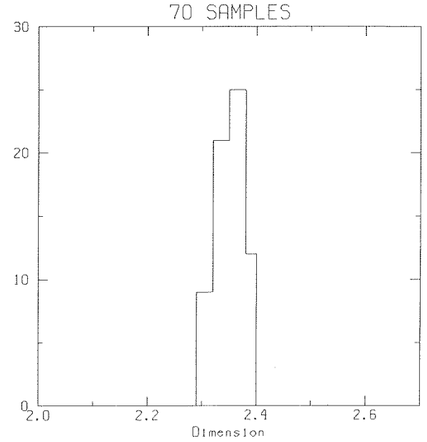

Fig. 11. Histogram of the inferred fractal dimension of the interface obtained from 70 visualizations in sections shown in Fig. 1a and b; the mean value is 2.36 ± 0.03

The algorithm for computing the fractal dimension has been described elsewhere (e.g., Sreenivasan and Meneveau 1986), and is only briefly outlined here. The entire image is covered with boxes of a given size ε, and the number of boxes that contain the boundary $N(\varepsilon)$ is counted. The procedure is repeated for many different values of ε. The number of boxes containing the interface in general increases with increasing resolution, following a power law $N(\varepsilon) \sim \varepsilon^{-D}$, where D is the fractal dimension of the boundary. The value of D as determined from the negative slope of a log-log plot of $N(\varepsilon)$ vs ε (a typical one is shown in Fig. 10) turns out to be 1.36. Orthogonal sections also yielded 1.36 within the experimental error, showing the independence of the result on the orientation of the intersecting plane. Figure 11 shows a histogram of the inferred fractal dimension of the interface obtained from 70 visualizations in two orthogonal directions. The mean value from this histogram was found to be 2.36 ± 0.03.

Another measure of the fractal dimension can be obtained from line intersections of the surface. In this case the dimension of the set of points where the line intersects the surface is 2 less than the dimension of the surface. The dimension of the surface determined from such intersections was also found to be 2.36, within experimental error.

5 Summary and discussion

It has been shown here that setting a proper threshold provides an adequate means for marking the scalar interface in

two-dimensional digital images of a turbulent flow. This threshold can be determined by one of two methods described in the text: Where the histogram of the pixel intensity is essentially bimodal, the threshold corresponding to the local minimum is the appropriate one, while in all other cases the one corresponding to the change in slope of the thresholded average intensity curve provides an adequate value. The use of the gradient and Laplacian operators, which intuitively can be thought of as sharpening the edges, do not work well primarily because of the large intensity variations within the scalar-marked region itself. To make these methods work, introduction of artificial parameters akin to the hold-time in one-dimensional time cuts becomes necessary.

The threshold determination becomes increasingly uncertain with increasing background noise level. Since it was shown above that it can be determined unambiguously for images obtained in the present system, it is helpful to provide an estimate of its overall noise level as a guide to what may be considered tolerable. Noise in instrumentation systems such as the one used here comes from a number of sources such as stray light scattered by particles in the ambient tank fluid (even though minimized by the use of an optical filter as well as several filters for tank water) and finite digital resolution both of pixel size and intensity. A direct and accurate estimate of the effective noise level is difficult. Here, it is estimated according to the procedure set forth by Bilger et al. (1977) in the context of cold wire signals.

It is clear that the histogram peak in Fig. 4 corresponding to the background intensity would be a Dirac delta function in the total absence of noise, but in practice it acquires a finite width by virtue of convolution with the superimposed noise. Bilger et al. showed that the peak region could be fitted by a Gaussian whose standard deviation would be a measure of the noise level. In the present example, it was indeed possible to fit a Gaussian roughly to this peak with a standard deviation of about 65 in the same units in which the maximum variability in the pixel intensity is 4,096. This gives a noise/signal ratio of about 1.3%. This noise level is not small compared to that attained in many cold wire signals. It is therefore believed that, if anything, the methods proposed here for choosing the threshold must work better in the cold wire records of temperature fluctuations in heated turbulent flows.

Acknowledgements

The authors wish to thank S. Majumdar and C. Meneveau for helpful discussions. This work was supported in part by a grant from DARPA and AFOSR.

References

Antonia, R. A. 1981: Conditional sampling in turbulence measurements. Ann. Rev. Fluid. Mech. 13, 131–156

Antonia, R. A.; Atkinson, J. D. 1974: Use of a pseudo-turbulent signal to calibrate an intermittency measuring circuit. J. Fluid Mech. 64, 679–699

Antonia, R. A.; Prabhu, A.; Stephenson, S. E. 1975: Conditionally sampled measurements in a heated turbulent jet. J. Fluid Mech. 72, 455–480

Bilger, R.; Antonia, R. A.; Sreenivasan, K. R. 1977: The determination of the intermittency for the probability density function of a passive scalar. Phys. Fluids 19, 1471–1474

Bradshaw, P.; Murlis, J. 1973: On the measurement of intermittency in turbulent flows. Imperial College Aero. Techn. Rep. 73–108

Canny, J. 1986: A computational approach to edge detection. IEEE Trans. 8, 679–698

Castleman, K. R. 1979: Digital image processing. Englewood Cliffs/NJ: Prentice Hall

Dimotakis, P. E.; Lye, R. C. M.; Papantoniou, D. A. 1983: Structure and dynamics of round turbulent jets. Phys. Fluids 26, 3185–3192

Hedley, T. B.; Keffer, J. F. 1974: Turbulent/non-turbulent decisions in an intermittent flow. J. Fluid Mech. 64, 625–644

Hesselink, L. 1988: Digital image processing in flow visualization. Ann. Rev. Fluid Mech. 20, 421–485

Kovasznay, L. S. G.; Ali, S. F. 1974: Structure of turbulence in the wake of a heated flat plate. Proc. 5th Int. Heat Transfer Conf., Tokyo, pp. 99–103

Mandelbrot, B. B. 1983: The fractal geometry of nature. New York: Freeman

Marr, D. M.; Hildreth, E. 1980: Theory of edge detection. Proc. R. Soc. Lond. Ser. B 207, 187–217

Rosenfeld, A.; Kak, A. C. 1982: Digital picture processing, 2nd edn. New York: Academic Press

Sreenivasan, K. R.; Antonia, R. A.; Stephenson, S. E. 1978: Conditional measurement in a heated axisymmetric turbulent mixing layer. AIAA J. 16, 869–872

Sreenivasan, K. R.; Meneveau, C. 1986: The fractal facets of turbulence. J. Fluid Mech. 173, 357–386

Sreenivasan, K. R.; Prasad, R. R. 1988: The fractal dimension of scalar surfaces in turbulent jets. Fluid Dyn. Trans. 14, 1–13

Sunyach, M.; Mathieu, J. 1969: Zone de mélange d'un jet plan fluctuations induites dans le cone à potentiel-intermittence. Int. J. Heat Mass Trans. 12, 1679–1697

Received July 25, 1988